Electronic Supplementary Material (ESI) for CrystEngComm.

Supplementary Information

Cubic ZnP_2 nanowire growth catalysed by bismuth

Seung Hwan Oh and Yong Kim*

Department of Physics, Dong-A University, Hadan-2-dong, Sahagu,

Busan 49315, Korea

Corresponding Author

*E-mail: yongkim@dau.ac.kr

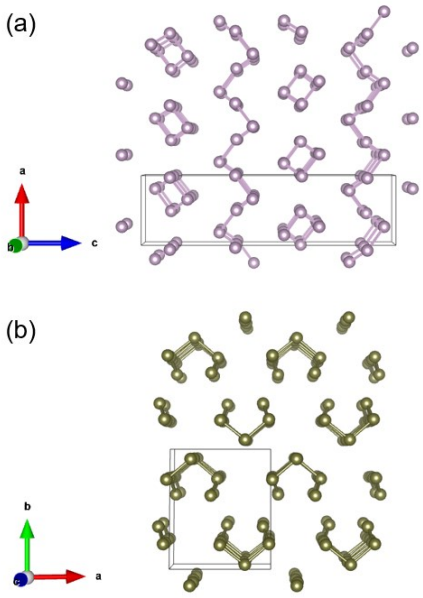

Fig. S1 (a) Infinite phosphorus chains which run along *a* and *b* axis found in tetragonal α-ZnP_2. (b) Open pentagonal phosphorus chains which run along *c*-axis in monoclinic β-ZnP_2. Atomic structures are simulated by VESTA 3.[1]

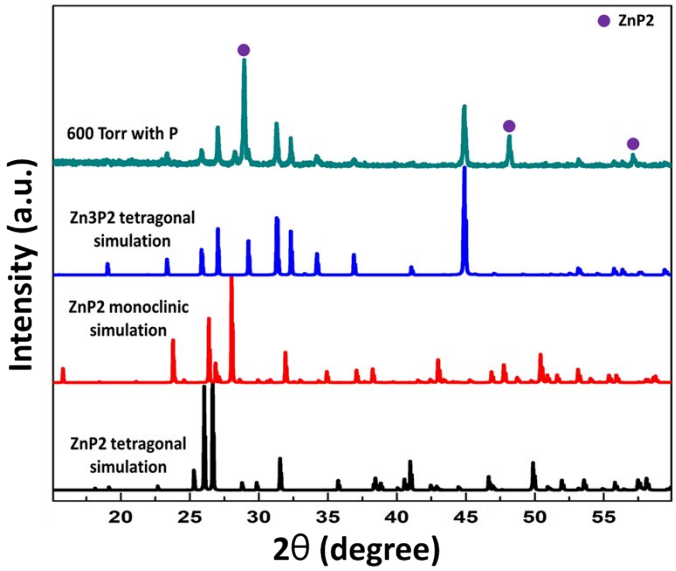

Fig. S2 X-ray diffraction spectrum of as-grown ZnP_2 nanowire sample grown at 600 Torr with extra phosphorus vapour. Simulated x-ray diffraction spectra of α-ZnP_2 tetragonal, β-ZnP_2

monoclinic, and α-Zn_3P_2 tetragonal structures for comparison. X-ray diffraction spectra are simulated by VESTA 3.[1] Closed circles are exceptional reflections which do not match to the simulated spectra of α-Zn_3P_2 tetragonal structure.

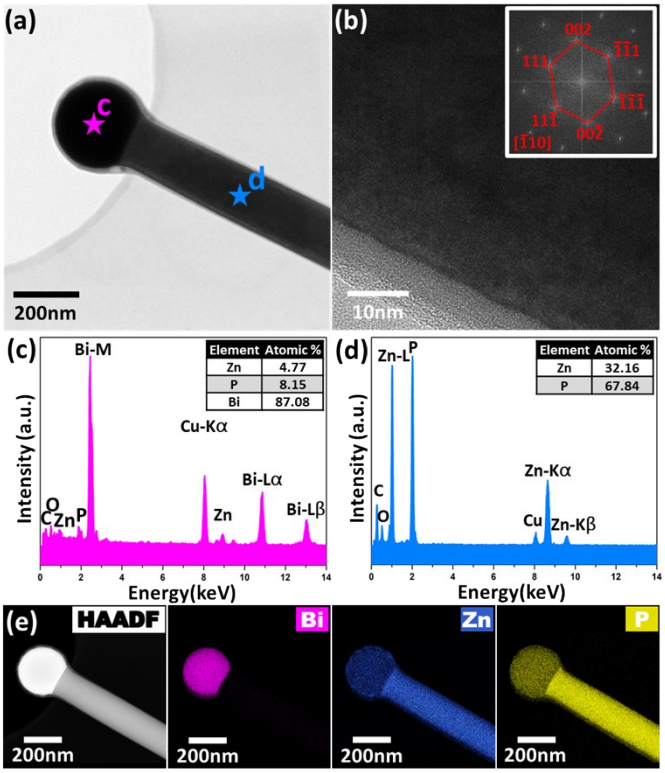

Fig. S3 (a) TEM image of a γ-ZnP_2 nanowire (diameter = 160 nm) grown at 100 Torr with extra phosphorus vapour. The nanowire was chosen in the same TEM grid as in Figure 4. Solid stars represent the positions subjected to EDX analysis. (b) High-resolution TEM image and power spectrum of a lattice image with Miller index assignments. Zone axis was $[\bar{1}10]$. (c) EDX profile of the catalyst with [Bi] = 87.1 atomic %. (d) EDX profile of the nanowire with [Zn]/[P] = 0.47. (e) HAADF STEM image and EDX elemental mapping of the nanowire for bismuth, zinc, and phosphorus.

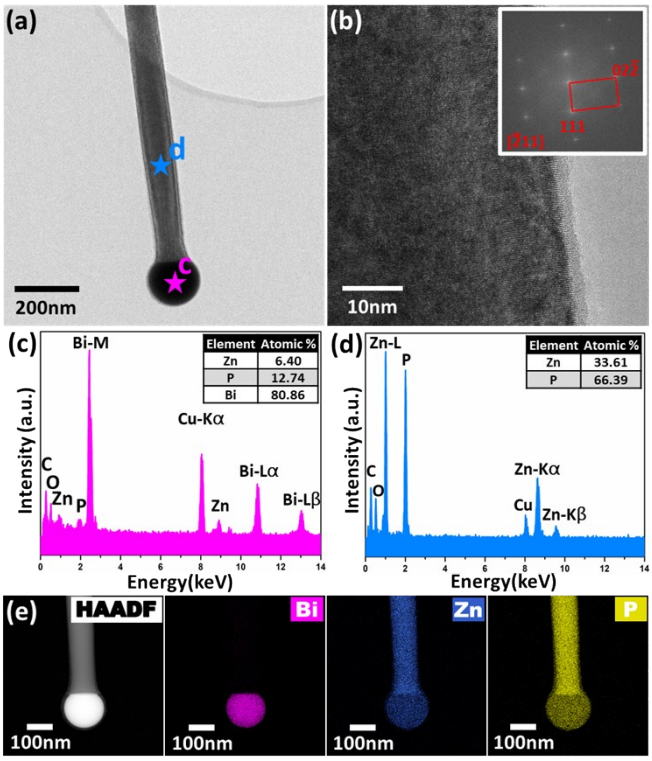

Fig. S4 (a) TEM image of a γ-ZnP_2 nanowire (diameter = 95 nm) grown at 100 Torr with extra phosphorus vapour. The nanowire was chosen in the same TEM grid as in Figure 4. Solid stars represent the positions subjected to EDS analysis. (b) High-resolution TEM image and power spectrum of a lattice image with Miller index assignments. Zone axis was $[\bar{2}11]$. (c) EDX profile of the catalyst at [Bi] = 80.9 atomic %. (d) EDX profile of the nanowire with Zn/P = 0.51. (e) HAADF STEM image and EDX elemental mapping of the nanowire for bismuth, zinc, and phosphorus.

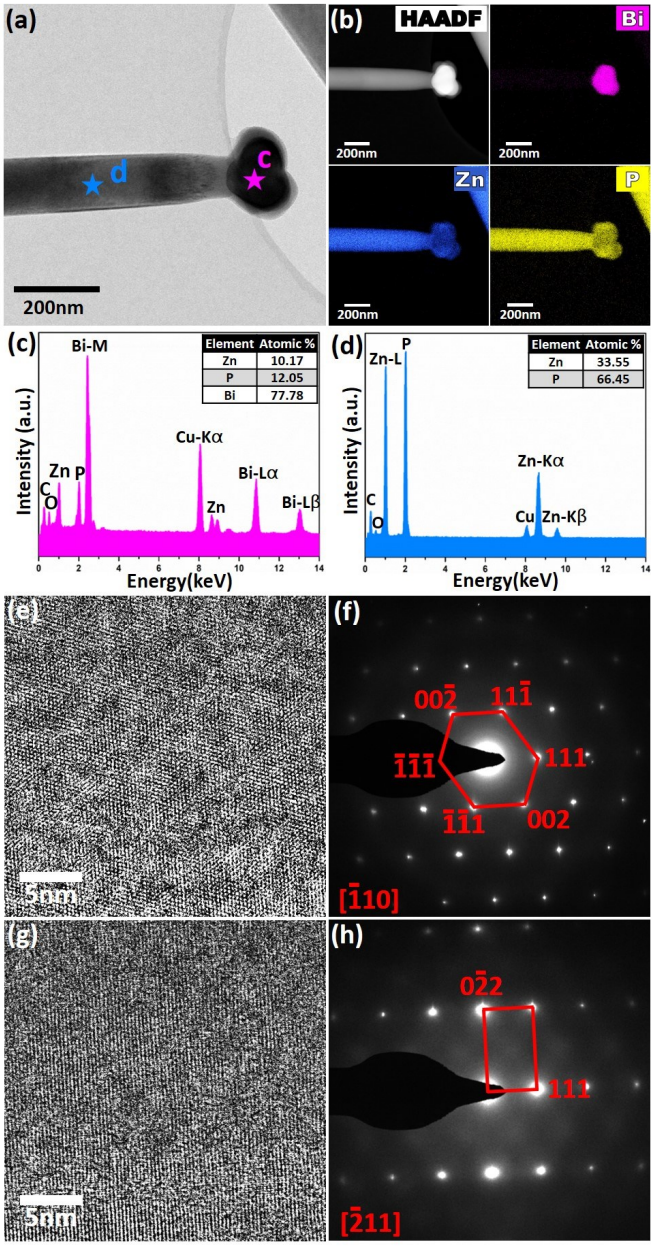

Fig. S5 (a) TEM image of a γ-ZnP_2 nanowire (diameter = 130 nm) grown at 600 Torr with extra phosphorus vapour. Solid stars represent the positions subjected to EDX analysis. (b) HAADF STEM image and EDX elemental mapping of the nanowire for bismuth, zinc, and phosphorus. (c) EDX profile of the catalyst at the position with [Bi] = 77.8 atomic%. (d) EDX profile of the nanowire

at [Zn]/[P] = 0.50. (e) High-resolution TEM image. (f) SAED pattern with Miller index assignments. Zone axis was $[\bar{1}10]$. (g) High-resolution TEM image after rotating on an axis of the nanowire by 30°. (h) SAED pattern with Miller index assignments. Zone axis was $[\bar{2}11]$.

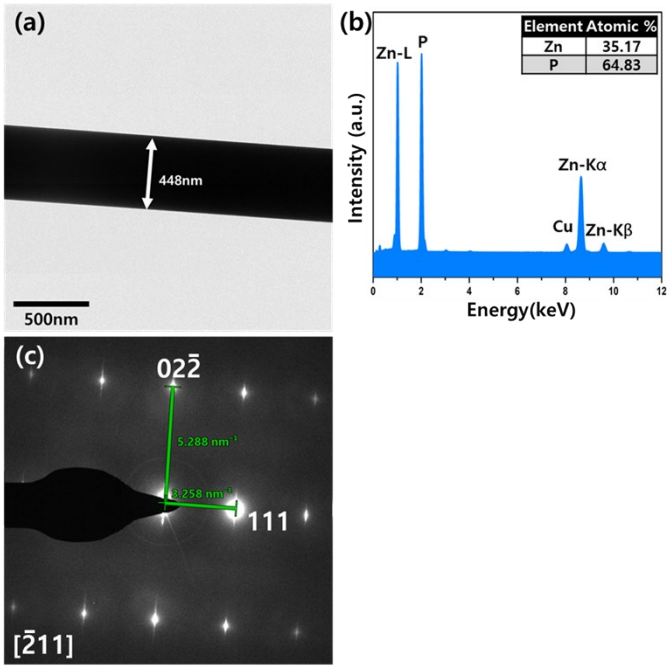

Fig. S6 (a) TEM image of a γ-ZnP_2 nanowire with exceptionally large diameter (= 448 nm) grown at 600 Torr with extra phosphorus vapour. (b) EDX profile of the nanowire. Note that [Zn]/[P] = 0.54. (e) Selective area electron diffraction pattern showing cubic γ-ZnP_2 phase. Zone axis was $[\bar{2}11]$.

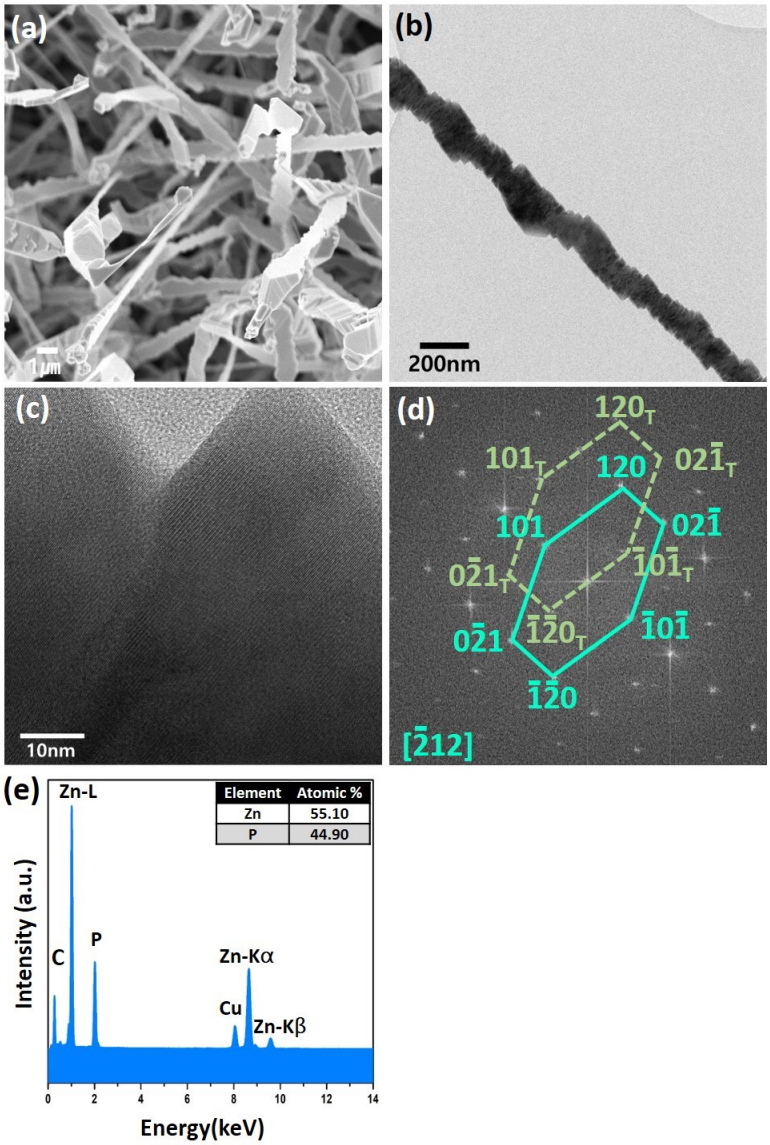

Fig. S7 (a) FESEM image of a Zn_3P_2 nanowire catalysed by gold grown at 100 Torr with extra phosphorus vapour. (b) TEM image of the defective nanowire (c) High-resolution TEM image. (d) Power spectrum with Miller index assignments. Zone axis was $[\bar{2}12]$. Note that twining reflections are denoted by subscript T. (d) EDX profile of the nanowire. Note that [Zn]/[P] = 1.2.

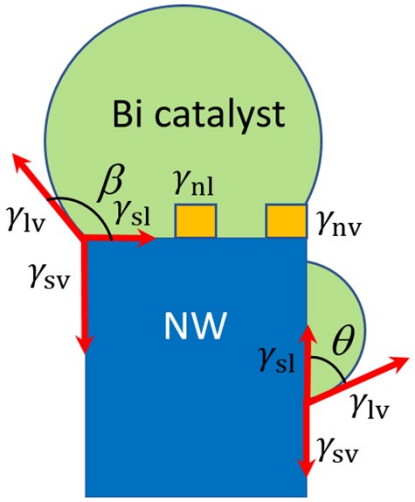

Fig. S8 Schematic nucleation models for Zn_3P_2/ZnP_2 nanowires in molten bismuth catalyst. Two possible nucleation events at centre and triple phase boundary are depicted. β is the contact angle and θ is the contact angle when catalyst forms at the side wall. γ_{ls}, γ_{lv}, γ_{sv}, γ_{nl}, and γ_{nv} are the surface energies of solid–liquid, liquid–vapour, solid–vapour, nucleus–liquid, and nucleus–vapour, respectively.

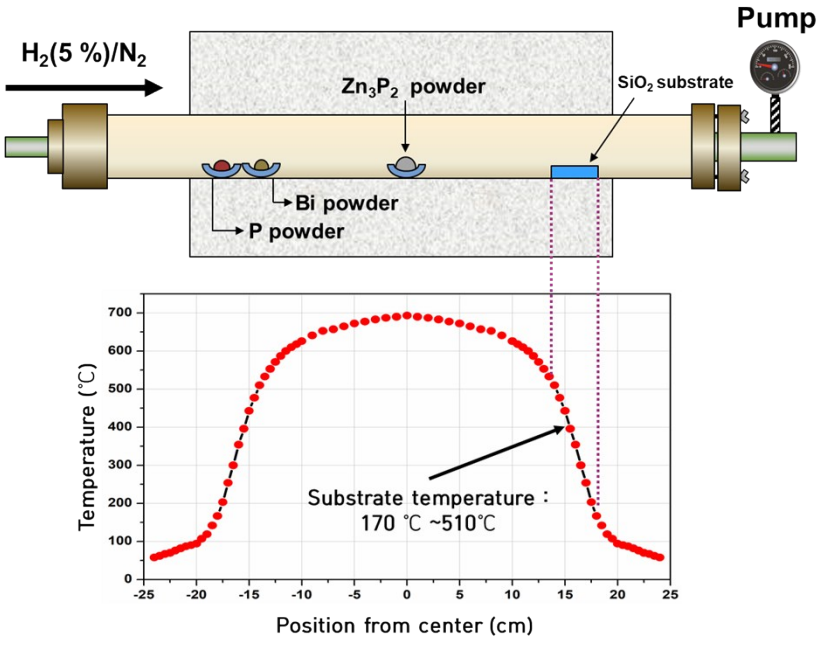

Fig. S9 Physical vapour transport system and temperature profile.

REFERENCES

(1) K. Homma and F. Izumi, *J. Appl. Crystallogr.*, 2011, **44**, 1272−1276.